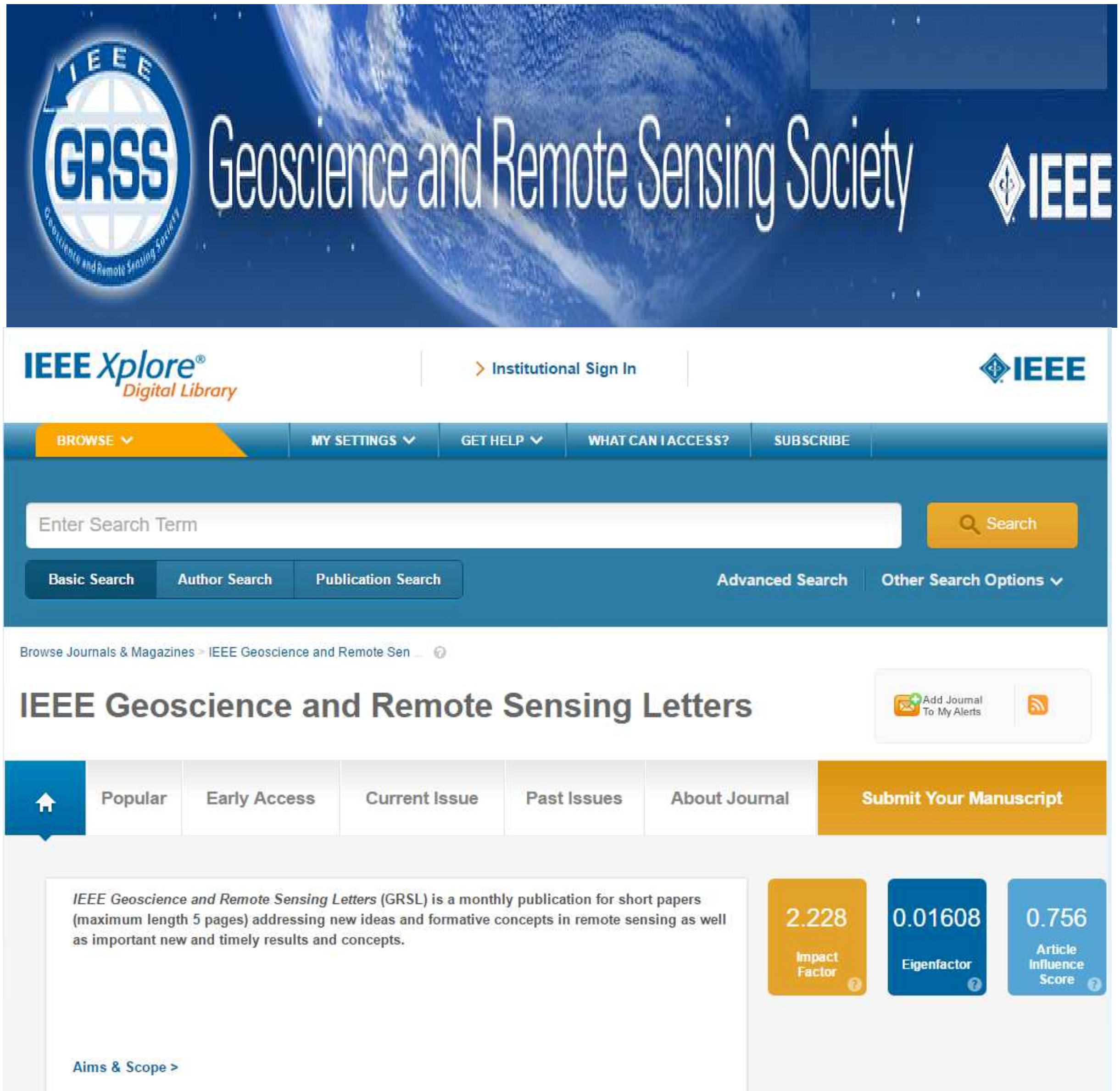

SELLAOUTI Aymen

HAMOUDA Atef

DERUYVER Aline

WEMMERT Cedric

Template based hierarchical building extraction

GEOSCIENCE AND REMOTE SENSING LETTERS

Pavia, Italy, 4 August 2013

To whom it may concern

I hereby certify you that the paper

GRSL-00125-2013.R2
Template based hierarchical building extraction
by Sellaouti, Aymen (contact); Deruyver,Aline; Wemmert, Cédric; Hamouda, Atef

was accepted for publication in the IEEE Geoscience and Remote Sensing Letters **on Aug. 2, 2013**, and will be printed in next available issue.

Sincerely,

Paolo Gamba

Prof. Paolo Gamba
Editor in Chief, *IEEE Geoscience and Remote Sensing Letters*
University of Pavia, Italy
paolo.gamba@unipv.it

Template-Based Hierarchical Building Extraction

Aymen Sellaouti, *Student Member, IEEE*, Atef Hamouda, Aline Deruyver, and Cedric Wemmert

***Abstract*—Automatic building extraction is an important field of research in remote sensing. This letter introduces a new object-based building extraction approach. So far, many object-based algorithms for building extraction have been proposed. However, these algorithms mainly operate in two phases: object construction and building extraction. The majority of these algorithms heavily relies on the object construction process, mainly due to the lack of interaction between the two steps. To overcome these drawbacks, we introduce a new hierarchical approach based on building templates. Carried out experiments on data sets of images from the urban area of Strasbourg show the benefits of our approach.**

***Index Terms*—Building, cooperation, dynamic template, object-based.**

I. Introduction

FOR more than 20 years, building extraction from digital images has been one of the most complex and challenging task faced by computer vision and photogrammetry communities. Toward making building extraction process more efficient, the dedicated literature is a witness of attempts in automating the extraction processes [1]–[5]. Object-based building extraction is one of the most promising fields of research. This approach is based on an object-based image analysis (OBIA) [6], that was developed in order to bridge the gap between the increasing amount of detailed geospatial data and the complex features recognition. OBIA for building extraction is usually composed of two steps; object construction and building identification. Lari and Ebadi [1] proposed an automated building extraction system based on neural networks (NN) system. Aminipouri *et al.* [7] proposed an object-based approach to create an accurate inventory of buildings. They started by a combination of Chessboard and Multi-Resolution segmentation to extract the regions in the image using the eCognition software. The classification was done using fuzzy membership functions and refined with an NN classifier. Singh *et al.* [8] used an NDVI-based segmentation and morphological operations. After the segmentation step, the authors used morphological operations to separate the roads from building regions on the bases of their spatial properties. To sum up, most of the aforementioned approaches showed the same limitations: the identification step is in a snugness connection with the extraction one. In fact, if objects are badly constructed, buildings cannot be accurately identified. To tackle this issue, we introduce a hierarchical region-based extraction approach. The aim of this letter is to present a collaborative segmentation classification approach for building extraction. A hierarchical growth is used based on a building template to identify the growth region. The letter is organized as follows: Section II introduces our proposed method. Section III highlights some experiments. Conclusions are provided in Section IV.

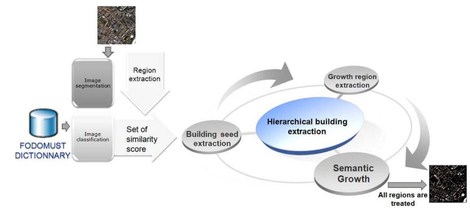

Fig. 1. Hierarchical building extraction sketch.

II. Hierarchical Building Extraction

In this section, we introduce the proposed approach, which aims at improving building extraction based on expert knowledge. In fact, the expert knowledge is a very important source of information in the recognition and classification of images. They can be an important factor in the decision between two ambiguous classes or even a primary source for systems analysis. The expert knowledge used in this approach are extracted from a geographical dictionary built during the FODOMUST project [9]. This dictionary is a textual document describing the different classes of the image using textual (e.g., buildings have rectangular shape) and numerical (e.g., building area in [50; 60]) descriptions for the different attributes describing each class. The numerical knowledge are represented by an ontology made up of a hierarchy of concepts having a label (e.g., building) and defined by a set of attributes (e.g., area, permiter) which are associated to an interval of accepted values (e.g., [MinValue; MaxValue]). This approach is split into two steps as depicted by Fig. 1. The first step is a preprocessing one which aims at preparing data for the following step. This allows the decomposition of the image into a set of homogeneous objects based on low-level features such as radiometry. Then, we classify the image by calculating a score for each region based on low-level features provided by the expert. This score introduces the notion of confidence that provides a degree of validity of the labeling of each object and so allowing

Manuscript received February 8, 2013; revised June 3, 2013 and July 12, 2013; accepted August 2, 2013. Date of publication August 26, 2013; date of current version November 25, 2013.

A. Sellaouti is with the Laboratory of Computing in Programming, Algorithmic and Heuristic, Faculty of Sciences of Tunis, Campus Universities Tunis, 1007 Tunis, Tunisia and also with Engineering, Computer and Imaging Sciences Laboratory, University of Strasbourg, 67400 Strasbourg, France (e-mail: aymen.sellaouti@icube.unistra.fr).

A. Hamouda is with Laboratory of Computing in Programming, Algorithmic and Heuristic, Faculty of Sciences of Tunis, Campus Universities Tunis, 1007 Tunis, Tunisia (e-mail: atef_hammouda@yahoo.fr).

A. Deruyver and C. Wemmert are with Engineering, Computer and Imaging Sciences Laboratory, University of Strasbourg, 67400 Strasbourg, France (e-mail: Aline.Deruyver@lsiit.u-strasbg.fr; wemmert@unistra.fr).

Color versions of one or more of the figures in this paper are available online at http://ieeexplore.ieee.org.

Digital Object Identifier 10.1109/LGRS.2013.2276936

the designing of a growth hierarchy. The second step is the hierarchical building extraction based on expert knowledge.

A. Preprocessing

The preprocessing is a data preparation step, which aims at extracting a set of regions to which we attribute a confidence score. It is split into two steps: segmentation and classification. The proposed approach is an object-based approach. To converge from pixel based to object-based image vision, we have to proceed to an object construction phase. The more often used process for object construction is segmentation. In our approach, the first segmentation allows us to extract homogenous objects from the image according to low level features (e.g., radiometry). These objects will play the role of seeds and candidates regions all along the growth hierarchy in the second step. The chosen algorithm has to fulfill the criterion of over-segmentation. Indeed, given the properties of region growing algorithms, which are based on the fusion of fragments of an object to be detected, it is clear that a sub-segmentation of the image implies the loss of some objects. We have chosen the watershed algorithm that easily allows an over-segmentation of the image [9]. The classification step aims at assessing the region membership for each class of the image. For that purpose, any kind of classification can be used, the final output must be a set of score rating the membership of the correspondant region to the image classes with or without using expert knowledge. For our approach, we propose a classification based on a confidence score. This score reflects the validity of the regions based on the knowledge provided by the expert. We use the similarity score proposed by Forestier *et al.* [9]. This score relies on an attribute-oriented approach as it uses low-level knowledge of the image that are formalized in the form of low-level descriptors. The proposed similarity score is used to check the validity of the attribute values of a region with respect to the intervals defined by the expert. The expert provides an interval containing the minimum value and the maximum value that can take each attribute for each class. The similarity score compares the attributes values of a region with the attributes values of the object to classify.

Note 1—(Region): Let R be the set of regions obtained from segmentation. $R = \{r_i\}_{i\in[1,N_R]}$ where N_R represents the cardinality of R.

Note 2—(Class): Let C be the set of classes in the image. $C = \{c_j\}_{j\in[1,N_C]}$ where N_C denotes the cardinality of C.

Note 3—(Attribute): Let A be the set of features identifying a class. $A = \{a_k\}_{k\in[1,N_k]}$ where N_k is the cardinality of A.

Definition 1—(Validity Degree): Let $Valid(a, c_j, r_i)$ the degree of validity between a class c_i and a region r_i for a given attribute a_k and let $v(r_i, a_k)$ be the value of the attribute a_k for the region r_i

$$Valid(a, c_j r_i) \times \begin{cases} 1; & v(r_i,a_k) \in [min(c_j,a_k), max(c_j,a_k)] \\ \frac{v(r_i,a_k)}{min(c_j,a_k)}; & v(r_i,a_k) < min(c_j,a_k) \\ \frac{max(c_j,a_k)}{v(r_i,a_k)}; & v(r_i,a_k) > max(c_j,a_k). \end{cases} \quad (1)$$

Definition 2—(Similarity Score): The similarity score $Sim(r_i, c_j)$ is computed according to the validity between the region r_i and the class c_j of each attribute weighted by a weight $w(k, c_j)$

$$Sim(r_i, c_j) = \frac{\sum_{a\in A} w(a_k, c_j) Valid(a_k, c_j, r_i)}{\sum_{a\in A} w(a_k, c_j)}. \quad (2)$$

Definition 3—(Set of Similarity): We define the similarity set as all the similarity scores of any region $r_i \in R$ with respect to any class $c_j \in C$

$$SIM = \{Sim(r_i, c_j) | r_i \in R \; et \; c_j \in C\}. \quad (3)$$

B. Growing Process to Detect Buildings

This is the main step of the approach. It is an iterative process which allows to build the growth hierarchy based on the sets of regions R, the set of classes C, the set of similarity scores SIM and the confidence scores obtained for each region. Buildings have specific properties that differentiate them from other classes. Indeed, buildings sharply contrast with their neighbors. They also have the property to be homogenous, this is due to a cultural characteristic of Strasbourg city (France) which imposes specific characteristics for building construction like roofs' angles, construction materials and colors. Most buildings do not contain vegetation. Buildings usually have linear and regular contours [10]. The other expert knowledge was extracted from FODOMUST that represents a set of high and low level expert knowledge like area, perimeter, height, width, etc. Using these properties and the detected confident building seeds, we propose a hierarchical growth for building extraction. The designing of the hierarchy is preceded by a calculation based on the similarity scores as it is explained in the following [11]–[13].

Definition 4: For a region $r_i \in R$, we define the set of classes that maximize the similarity score $Sim(r_i, c)$ among all the classes $c \in C$. We denote by $\delta(r_i)$ this set

$$\delta(r_i) = \arg\max_{c\in C} Sim(r_i, c). \quad (4)$$

Definition 5: For each region $r_i \in R$, we define $S_{max}(r_i)$ and $C_{max}(r_i)$, respectively as follows:

$$C_{max}(r_i) = \begin{cases} random\,(\delta(r_i)) & \text{if } |\delta(r_i)| > 1 \\ \delta(r_i) & \text{otherwise} \end{cases} \quad (5)$$

$$S_{max}(r_i) = \begin{cases} Sim\,(r_i, C_{max}(r_i)) & \text{if } |\delta(r_i)| == 1 \\ 0 & \text{otherwise.} \end{cases} \quad (6)$$

$S_{max}(r_i)$ represents the maximum similarity score of the region r_i for all classes of C. In the case where $\delta(r_i)$ has more than one class, then we deduce that there is a confusion i.e., *this region is no longer a trustworthy region but a conflictual one*. In this case, $C_{max}(r_i)$ takes arbitrarily one of the classes of $\delta(r_i)$ and $S_{max}(r_i)$ is assigned to 0. If $\delta(r_i)$ contains a single value, then it will be assigned to $C_{max}(r_i)$ and $S_{max}(r_i)$ will be the similarity score $Sim(r_i, C_{max}(r_i))$ of the class C_{max} for the region r_i. The computation of C_{max} and S_{max} serves as a basis for the iterative algorithm of hierarchical growth.

As introduced by algorithm 1, each iteration k of the growth process is composed of three steps: 1) the extraction of building seed's of each iteration which are the regions not yet treated having the highest similarity score; 2) the growing area extraction using the geometric properties of buildings extracted from FODOMUST dictionary; and 3) growth based on expert knowledge and constrained by the regions already treated (e.g., in the iteration m with $k > m > 0$) and the seeds of the same iteration but not belonging to the buildings.

Algorithm 1: Growth algorithm

Input: R the set of regions of the image obtained by segmentation, SIM the set of similarity scores for the regions of the image.
Output: candidates the set of candidates to be seed, Seed the set of seeds and fusion the set of merged regions.

Begin
  $candidates_0 = R$, $k = 1$, $Sconstraint = \emptyset$;
  while $candidates_{k-1} \neq \emptyset$ **do**
    $Seed_k = \arg\max_{r \in candidates_{k-1}} S_{max}(r)$
    $Sbuilding_k = \{r \in Seed_k | Cmax(r) = building\}$
    $Sconstraint_k = \{Seed_k \setminus Sbuilding_k\}$
    $Sconstraint = \{Sconstraint \cup Sconstraint_k\}$
    $fusion\_building_k = \{r \in candidates_{k-1} \setminus Seed_k | r \text{ merged in level } k\}$
    $candidates_k = \{candidates_{k-1} \setminus fusion\_building_k \cup Seed_k\}$
    $k = k + 1$
  endw
End

---

1) Building Seeds' Selection: The building seeds' selection allows to extract the most confident building region from the candidates in each iteration. It consists in the extraction of all seeds of level k from the set $candidates_{k-1}$ of the regions not already processed in the previous levels of the hierarchy and belonging to the class building. The seeds, extracted at this level, are the regions r_i that maximize $S_{max}(r_i)$ among all candidate regions of this level, i.e.,

$$Seeds_k = \arg\max_{r \in candidates_{k-1}} S_{max}(r). \tag{7}$$

Also, we decompose $Seeds_k$ into two sets, $Sbuilding_k$ that contains the seeds of class building and $Sconstraint_k$ that contains the seeds of other classes

$$Sbuilding_k = \{r \in Seeds_k | C_{max}(r) = building\} \tag{8}$$

$$Sconstraint_k = \{Seed_k \setminus Sbuilding_k\}. \tag{9}$$

2) Growing Area Extraction: Expert knowledge, given by the FODOMUST dictionary, constitute an important amount of information which helps to extract buildings. The major problem is how to integrate this knowledge within our process. We propose to use this knowledge in two steps which are the growing area extraction and the semantic growth. To define the growing area for each seed of level k, we create a building template based on the information about height, width, area and shape extracted from FODUMUST dictionary. For a given building and considering that the main building shape is rectangular, we simulate all the possible solutions by projecting the created template according to 360° angles in order to intersect

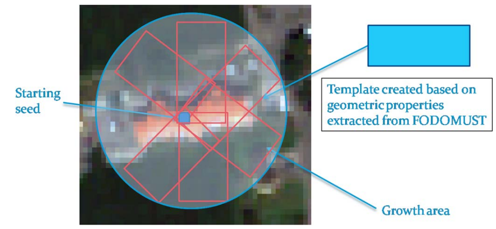

Fig. 2. Growth building template creation.

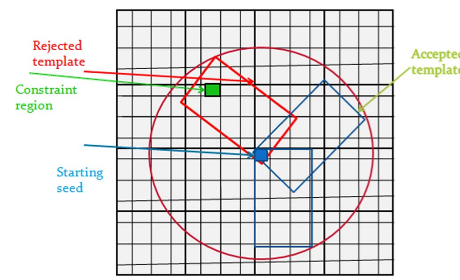

Fig. 3. Template: Acceptation and rejection.

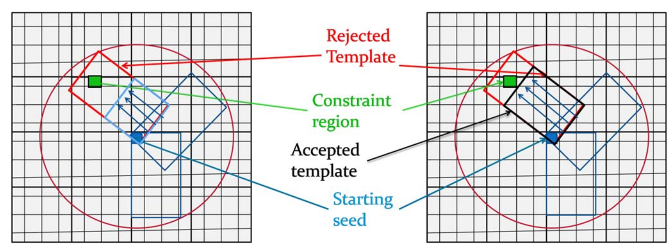

Fig. 4. Dynamic creation of the growth template.

the candidate regions for the growing process. The simulation is done by using the confident building seeds of the current level, i.e., extracted by the selection seeds step and the set of extracted building segments of the previous levels of the hierarchy. The center of the circular projection will be the treated seed. Fig. 2 illustrates how we select the candidate regions. In order to limit the growth area, this method can be generalized to any geometrical shape. The only difference is that the template must be modeled according to the shape of the object to be detected.

To prune the regions based on the constraints extracted in each iteration, we reject the template which contains a constraint region. As illustrated in Fig. 3, the red template is not selected because it contains a constraint region (the green one). After finding all the accepted templates for the current seed, we used the pixels delineated by these templates as the possible growing area of the current seed.

The limitations of this method is that the whole template is pruned, that may eliminate some true candidate regions. To solve this problem, we improve the template generation by making it dynamic, i.e., for each angle, instead of tacking the whole template area, we only take the part of template which does not contain any constraint region. This means that the template starts from the seed and grows until the first encounter of a constraint. Fig. 4 shows how we create dynamic template.

3) Semantic Growth: After delineating the growing area based on the template-based process described before, we start the semantic growing step in order to locate the final building. The semantic growth is based on expert knowledge extracted from FODOMUST. The region growing process starts from each seeds of level k. This process is based on a growing algorithm that allows merging each seed with its neighboring regions based on a set of homogeneity criteria. This fusion is limited by the growing area defined by the previous treatment and it is constrained by a set of expert building knowledge and a set of rules specific to the hierarchy. It manages the integration of constraints within the hierarchy. Indeed, a seed of level k cannot change the state of a seed of a lower level. To evaluate which neighbor will be merged with the building seed, we computed a fitness function based on the expert knowledge. This function is knowledge dependent, its role is to reflect the expert knowledge by guiding the growth process according to these knowledge. The implementation of this function can be generalized to any kind of knowledge by providing a numeric rating to each knowledge. The fitness function associates with each region (made up of the seed region and the neighbor candidate) a real value to measure its quality. In this letter, our aim is to design a function that can provide an optimal growth to each building seed. To define this function [(10)], we based our work on a set of expert knowledge describing buildings (area, rectangularity and homogeneity)

$$\mathbb{F}(r) = \mathbf{A}rea \times \mathbf{R}_{GRE} \times \mathbf{H}om. \qquad (10)$$

Let r be the region to be evaluated. The area evaluation $\mathbf{A}rea$ is defined as follows as:

$$\mathbf{A}rea = \begin{cases} 1 & \text{if } area(r) \in [min_{area}, max_{area}] \\ \frac{area(r)}{min_{area}} & \text{if } area(r) < min_{area} \\ \frac{max_{area}}{area(r)} & \text{if } area(r) > max_{area} \end{cases} \qquad (11)$$

with $area(r)$ standing for the area of the building (r) and min_{area}, max_{area}, respectively denoting the minimal and the maximal area of a building based on expert knowledge.

The rectangularity is a descriptive measure, that gives a clue about the shape of the object and how it is near to the rectangular shape. We based our work on the model provided by Hentati *et al.* [14], that uses the Radon transform to create a shape descriptor called GR-signature. After that, the authors used a new rectangularity metric R_{GRE} that provides the rate of rectangularity of objects. In fact, this metric measures the difference in the matching between the object's GR-signature and a perfect rectangle shape GR-signature. The formula of the R_{GRE} is written as follows:

$$R_{GRE} = \frac{\theta_{measure} + A_{measure}}{2} \qquad (12)$$

where $A_{measure}$ is the normalized measure of the amplitude shift and the $\theta_{measure}$ is the normalized angular phase shift between both signatures.

The homogeneity is a factor that indicates the degree of the color similarity between the seed's pixels and the candidate's pixels. Thus, we define the homogeneity as follows:

$$\mathbf{H}om = 1 - (|Diff_r| + |Diff_g| + |Diff_b| \times 0.01) \qquad (13)$$

where $Diff_i$ is the difference between the mean of each band color of the seed pixels and the candidate pixels. In the eq (13), if the difference is equal to zero, then the homogeneity result is one. Otherwise, for each unit in the difference we reduce the homogeneity by 0.01 which stand to 1. The value 0.01 is a homogeneity threshold allowing to limit the growth to the regions that satisfy it. This value was experimentally computed. The Homogeneity evaluation $\mathbf{H}om$ measures the standard deviation of the region. The fitness function is varied to favor regions that have a high rectangularity with an area that belongs to the interval for specific buildings and a high homogeneity characterized by a relative low standard deviation. After defining the fitness function, we compute it for all the neighbors of the treated seed. For each neighbor, we evaluate the region created by the fusion between the seed and this neighbor. Then, we sort the set of the neighbors based on the fitness. If the value of the highest neighbor is greater than the value of the evaluation function of the seed, we merge the neighbor with the seed and we repeat this process until no neighbors merging can improve the evaluation of the seed building region.

(a) (b)

Fig. 5. Dense site extraction results. (a) Input image. (b) The extraction results.

Definition 6: $(fusion\_building_k)$ is defined by all the regions that have been merged in the level k with one of the seeds of $Sbuilding_k$

$$fusion\_building_k = \{r \in candidates_{k-1} | r \ has \ been \ merged \ in \ the \ level \ k\}. \qquad (14)$$

All candidate regions in the level $k+1$, denoted $candidates_k$, will be the set of candidates of the level k after the removal of parts merged regions and $Sbuilding$ and $Sconstraint$ of the level k

$$candidates_k = candidates_{k-1} \setminus \{fusion\_building_k \cup Sbuilding_k \cup Sconstraint_k\}. \qquad (15)$$

From this set, we reiterate in the same manner until exhaustion of the candidates.

III. Experiments

The study area is a Quickbird image covering urban areas of the city of Strasbourg (France), taken in 2008, having four bands, each one with a resolution of 2.44 m/px. We assess the proposed approach on a set of test area. The chosen examples exhibit different contexts existing in the image, i.e., the buildings had different orientation, density and sizes. We illustrate these results on three examples of test area. Fig. 5(a) depicts the dense area, the extracted buildings are shown in

(a) (b)

Fig. 6. Sparse site extraction results. (a) Input image. (b) The extraction results.

(a) (b)

Fig. 7. Mixed site extraction results. (a) Input image. (b) The extraction results.

TABLE I
QUANTITATIVE EVALUATION

sites	BCE	BPE	BNE	FA	BER	Exactness	Excellence %
site 1	251	27	17	17	85.08	93.65	80.44
site 2	367	22	20	20	89.73	94.83	85.54
site 3	85	7	8	5	85.00	94.44	80.95

Fig. 5(b). Fig. 6(a) presents a sparse area and Fig. 6(b) plots the map of the extracted buildings in the sparse context. In Fig. 7(a), a site, combining the sparse and dense contexts, is shown and the building extraction results is given in Fig. 7(b). Interestingly enough, the extraction results data highlight the robustness of the approach. In addition, the sparse site presents better extraction results thanks to the the noise reduction that increases in dense sites. In order to numerically assess the accuracy of our approach, we used the following metrics [15]: $BER = (BCE/(BCE + BPE + BNE)) * 100$, $Exactness = (BCE/BCE + FA) * 100$, $Excellence = (BCE/BCE + BPE + BNE + FA) * 100$, where BCE is the number of Building Correctly Extracted, BPE the number of Partially Extracted Buildings, BNE the number of Not Extracted Buildings and FA the False Alarms. The Building Extraction Rate (BER) assesses the object detection performance, measuring the rate of objects correctly denoted as buildings by our system. The Exactness is a measure of delineation performance, measuring the number of objects that are true buildings from the number of objects extracted as buildings. Finally, the Excellence percentage combines aspects of both measures to sketch the system performance. Table I introduces the obtained extraction rate for the three sites. It summarizes the value of the considered metrics for the three sites. We observed that these results prove the robustness of our approach. Indeed, the approach highlights good results for the three contexts and specially for the sparse one. However, we noticed some artifacts and non extracted buildings due to the classification during the pretreatment step.

IV. CONCLUSION

Object based approaches are frequently used for building extraction. However, they present the same drawback which is the object extraction dependency. To tackle this issue, we introduce in this letter a new object based building extraction approach which allows an interaction between object construction and extraction along the hierarchy. For each extracted seed, based on a confidence score, a template is dynamically generated to extract the growing area. Then, a growing process based on expert knowledge is used to extract the building. Despite the promising results of the approach, we plan to use meta learning to integrate new knowledge along the hierarchy and manage the choice of seeds.

REFERENCES

[1] Z. Lari and H. Ebadi, "Automated building extraction from high-resolution satellite imagery using spectral and structural information based on artificial neural networks," in *Proc. ISPRS Workshop*, Hannover, Germany, 2007, pp. 1–4.

[2] I. Sledge, J. Keller, W. Song, and C. Davis, "Conflation of vector buildings with imagery," *IEEE Geosci. Remote Sens. Lett.*, vol. 8, no. 1, pp. 83–87, Jan. 2011.

[3] A. Sellaouti, M. OuledSghaier, and A. Hamouda, "An edge-region cooperative multi-agent approach for buildings extraction," in *Proc. DICTAP*, Bangkok, Thailand, May 2012, pp. 51–60.

[4] B. Yang, Z. Wei, Q. Li, and J. Li, "Semiautomated building facade footprint extraction from mobile lidar point clouds," *IEEE Geosci. Remote Sens. Lett.*, vol. 10, no. 4, pp. 766–770, Jul. 2013.

[5] K. Stankov and D.-C. He, "Building detection in very high spatial resolution multispectral images using the hit-or-miss transform," *IEEE Geosci. Remote Sens. Lett.*, vol. 10, no. 1, pp. 86–90, Jan. 2013.

[6] T. Blaschke, "Object based image analysis for remote sensing," *Int. J. Photogramm. Remote Sens.*, vol. 65, no. 1, pp. 2–16, Jan. 2010.

[7] M. Aminipouri, R. Sliuzas, and M. Kuffer, "Object oriented analysis of very high resolution orthophotos for estimating the population of slum areas, case of dar es salaam, tanzania.," in *Proc. ISPRS XXXVIII Conf.*, Hannover, Germany, 2009, pp. 1–6.

[8] D. Singh, R. Maurya, A. Shukla, M. Sharma, and P. Gupta, "Building extraction from very high resolution multispectral images using ndvi based segmentation and morphological operators," in *Proc. Students Conf. Eng. Syst.*, 2012, pp. 1–5.

[9] G. Forestier, S. Derivaux, C. Wemmert, and P. Gançarski, "An evolutionary approach for ontology driven image interpretation," in *Proc. EvoWorkshops*, Boston, MA, USA, Jul. 2008, pp. 295–304.

[10] V. Poulain, "Fusion d'images optique et radar à haute résolution pour la mise à jour de bases de données cartographiques," Ph.D. dissertation, Inst. Recherche Inf. Toulouse, Nat. Polytech. Inst. Toulouse, Toulouse, France, Oct. 2010.

[11] A. Sellaouti, A. Hamouda, A. Deruyver, and C. Wemmert, "Hierarchical classification-based region growing (hcbrg): A collaborative approach for object segmentation and classification," in *Proc. 9th ICIAR*, Aveiro, Portugal, 2012, vol. 7324, pp. 51–60.

[12] A. Sellaouti, H. Rojbani, A. Hamouda, A. Deruyver, and C. Wemmert, "Hierarchical classification-based radon road extraction (hcbrre)," in *Proc. ICARCV*, Guanzhou, China, 2012, pp. 390–395.

[13] A. Sellaouti, A. Hamouda, A. Deruyver, and C. Wemmert, "Approche orientée objet sémantique et coopérative pour la classification des images de zones urbaines à très haute résolution," in *Proc. EGC*, Toulouse, France, 2013, pp. 103–114.

[14] J. Hentati, M. Naouai, A. Hamouda, and C. Weber, "Measuring rectangularity using gr-signature," in *Proc. 3rd MCPR*, 2011, pp. 136–145, Springer-Verlag, Berlin/Heidelberg, Germany.

[15] H. Rojbani, I. Elouedi, and A. Hamouda, "R-signature: A new signature based on radon transform and its application in buildings extraction," in *Proc. IEEE ISSPIT*, 2011, pp. 490–495.